

## ANOMALOUS X2-MODE ECRH POWER ABSORPTION AT THE TJ-II STELLARATOR: COMPARISON OF THEORY AND EXPERIMENTS

A.Y. POPOV, E.Z. GUSAKOV

Ioffe Institute, St. Petersburg, Russia

e-mail: [a.popov@mail.ioffe.ru](mailto:a.popov@mail.ioffe.ru)

The nonlinear phenomenon in inhomogeneous plasmas referred to as convective parametric decay instability (CPDI) has been intensively studied since the early 1970s [1,2]. The results of the analysis were summarized in the review [3]. Based on the developed model [1,2], the stability limits for microwaves used for electron cyclotron resonance heating (ECRH) in toroidal fusion devices were investigated, and the extremely high threshold of CPDI excitation, ranging from tens of MW to GW for various decay scenarios, was predicted [4]. This enabled the assertion that microwaves remain stable to any parametric decays in ECRH experiments operating with heating beams of up to megawatt power.

However, recent experimental observations, namely anomalous microwave emission in a frequency range shifted up and down with respect to the gyrotron frequency by about the lower hybrid frequency [5-9] and plasma emission at half-integer harmonics of the pump wave frequency [7,9] prove the nonlinear behavior of sub-megawatt microwave beams. The physical phenomena reported in [5-9] have been observed when a microwave pump beam passed through a plasma region with a non-monotonic density profile. As predicted by the low-threshold PDI model [10], in this case the low-threshold excitation of the most dangerous absolute PDI is possible. The latter manifests itself in the temporal growth of daughter waves, at least one of which is localized in the decay region due to the non-monotonic density and finite width of the microwave beam. This model allows giving a detailed quantitative explanation of the anomalous phenomena observed in ECRH experiments at TEXTOR [11,12], ASDEX-Upgrade [13] and Wendelstein 7-X [14].

It should be noted that the X2-mode ECRH experiments have also shown a discrepancy between the launched and actually absorbed microwave power, as well as between the predicted and measured power deposition profiles, especially at a hollow density profile [15-17]. A possible explanation was given in [18], where it was shown that the low-threshold parametric decay of the pump wave in the local maximum of the density profile, often observed in X2-mode ECRH experiments, can lead to the appearance of a two-dimensionally localized upper hybrid (UH) wave and a daughter extraordinary wave running from the decay layer to the plasma edge. The primary instability is then saturated by a cascade of secondary decays into two-dimensionally localized UH and ion Bernstein (IB) waves. Depending on the number of steps in the cascade of secondary decays, there is either moderate or strong anomalous absorption of pump power by the daughter waves [10]. It seems rather obvious that in the case of strong anomalous absorption the daughter extraordinary wave, having gained a significant fraction of the pump power and propagating to the edge of the plasma, is absorbed far beyond the pump wave ECR layer. This can explain both the broadening of the pump power deposition and the lack of actually absorbed microwave power in the discharge central zone.

In this report, using the above theoretical approach [18] we consider the results obtained in X2-mode ECRH experiments at TJ-II and showing strong density dependence of the pump wave absorption efficiency [17]. Figure 1 shows the density profile depicted by the thick solid line. It possesses an off-axis local maximum caused by the electron pump-out effect typical for on-axis ECRH. The other parameters are taken as follows  $B_0=1$  T,  $T_{e0} = 1$  keV. For this density profile the one-dimensional dispersion curve of the daughter UH wave  $q_x$  ( $f_m=33.9$  GHz, the mode number is equal to  $m=38$ ) down - shifted by the pump wave number  $k_{0x}$  ( $f_0 = 53.2$  GHz) is shown by the thin solid line. The wave number  $k_{sx}$  of the daughter X1-mode is plotted by the dashed dotted line. In the region where dispersion curves are nearly tangent the decay resonance condition is fulfilled, i.e.,  $q_x - k_{0x} - k_{sx} \approx 0$ , and the PDI becomes possible. The daughter extraordinary wave being excited in the decay layer then propagates to the edge of the plasma. Figure 2 shows the dependence of the instability threshold on the chord averaged density. The larger the density value, the larger the instability threshold. This makes it possible to propose an explanation for the dependence of the pump wave absorption efficiency on the plasma density, which was observed at TJ-II (see figure 9 in [17]). As can be seen in figure 2, there is a cutoff in density at which the pump wave PDI becomes no longer possible for the heating power of 0.3-0.4 MW. The pump power absorption in this case occurs in the ECR layer as predicted by the linear theory. The primary instability saturates due to pump wave depletion and a one- or two-step cascade, depending on the density value, of subsequent decays of the primary UH wave into secondary and tertiary trapped UH waves and running IB waves. Analyzing this cascade process numerically, one can calculate the power fraction gained by the daughter waves. Figure 3 shows the dependence of the power fraction gained by the daughter waves on the chord averaged density. At the density value  $n_0^{(1)}$  the transition from the PDI saturation regime with two-step cascade of secondary decays to the regime with one-step secondary decay takes place. The latter case corresponds to a

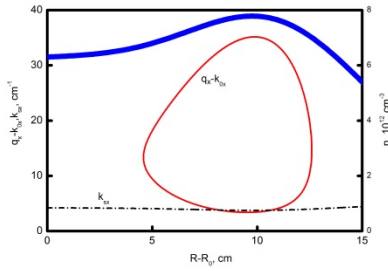


Figure 1. Right and bottom axes: the density profile is depicted by the thick solid line [17]. Left and bottom axes: the 1D dispersion curve of the daughter UH wave ( $f_m=33.9$  GHz,  $m=38$ ) down - shifted by the pump wave number ( $f_0 = 53.2$  GHz) is shown by the thin solid line. The wave number of the daughter X1-mode is plotted by the dashed dotted line. The plasma parameters are as follows  $B_0=1$  T,  $T_{e0} = 1$  keV.

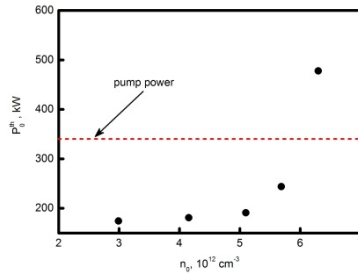


Figure 2. Dependence of the instability threshold on the chord averaged density value. The horizontal dashed line shows the typical power of a one microwave beam used in X2-mode ECRH experiments [17].

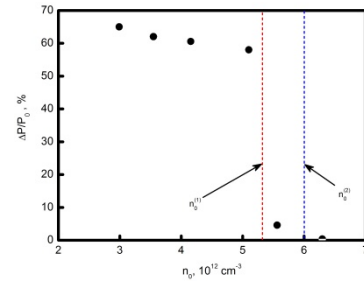


Figure 3. Dependence of the power fraction deposited to the daughter waves on the chord averaged density value. ( $n_0^{(1)}$  is the transition boundary from the mode with two-step decay cascade to the one-step cascade;  $n_0^{(2)}$  indicates the density PDI threshold at the pump power of 330 kW).

weak anomalous absorption [10], as it is seen in figure 3. The density value  $n_0^{(2)}$  is the transition boundary from a regime where the pump wave is unstable to a regime with the stable pump wave. As it is seen in figure 3, there is no anomalous absorption at density values greater than the cut-off value  $n_0^{(2)}$ .

Since the power deposition of all daughter the extraordinary and UH waves due to electron cyclotron damping is far from the region predicted for the pump wave, the anomalous absorption should broaden the total ECRH power deposition profile and reduce the measurable absorbed microwave power.

#### ACKNOWLEDGEMENTS

The analytical treatment is supported under the Ioffe Institute state contract FFUG-2024-0028 whereas the numerical modelling is supported under the Ioffe Institute state contract FFUG -2021-0003.

#### REFERENCES

- [1] ROSENBLUTH, M.N., Phys. Rev. Lett. **29** (1972) 565.
- [2] PILIYA, A.D., JETP Letters **17** (1973) 266.
- [3] REIMAN, A., Reviews of Modern Physics **51** (1979) 311.
- [4] COHEN, B.I., COHEN, R.H., NEVINS, W.M., ROGNLIEN, T.D., Reviews of Modern Physics **63** (1991) 949.
- [5] WESTERHOF, E., NIELSEN, S.K., OOSTERBEEK, J.W., SALEWSKI, M., DE BAAR, M.R., BONGERS, W.A., BÜRGER, A., HENNEN, B.A., KORSHOLM, S.B., LEIPOLD, F., MOSEEV, D., STEJNER, M., THOEN, D.J., Phys. Rev. Lett. **103** (2009) 125001.
- [6] NIELSEN, S.K., SALEWSKI, M., WESTERHOF, E., BONGERS, W., KORSHOLM, S.B., LEIPOLD, F., OOSTERBEEK, J.W., MOSEEV, D., STEJNER, M., Plasma Phys. Control. Fusion **55** (2013) 115003.
- [7] HANSEN, S.K., NIELSEN, S.K., STOBBER, J., RASMUSSEN, J., STEJNER, M., HOELZL, M., JENSEN, T., Nucl. Fusion **60** (2020) 106008.
- [8] TANCETTI, A., NIELSEN, S.K., RASMUSSEN, J., GUSAKOV, E.Z., POPOV, A.Y., MOSEEV, D., STANGE, T., SENSTIUS, M.G., KILLER, C., VECSEI, M., JENSEN, T., ZANINI, M., ABRAMOVIC, I., STEJNER, M., ANDA, G., DUNAI, D., ZOLETNIK, S., LAQUA, H., Nuclear Fusion **62** (2022) 074003.
- [9] CLOD, A., SENSTIUS, M.G., NIELSEN, A.H., RAGONA, R., THRYSSØE, A. S., KUMAR, U., S. CODA, NIELSEN, S.K., Physical Review Letters **132** (2024) 135101.
- [10] GUSAKOV, E.Z., POPOV, A.Y., Phys. Usp. **63** (2020) 365.
- [11] GUSAKOV, E.Z., POPOV, A.Y., Physics of Plasmas **23** (2016) 082503.
- [12] GUSAKOV, E.Z., POPOV, A.Y., Plasma Physics Reports **49** (2023) 949.
- [13] GUSAKOV, E.Z., POPOV, A.Y., TRETINNIKOV, P.V., Nucl. Fusion **59** (2019) 106040.
- [14] GUSAKOV, E.Z., POPOV, A.Y., Plasma Physics Reports **49** (2023) 194.
- [15] GUSAKOV, E.Z., POPOV, A.Y., MESHCHERYAKOV, A.I., GRISHINA, I.A., TERESHCHENKO, M. A., Phys. Plasmas **30** (2023) 122112.
- [16] EGUILIOR, S., CASTEJÓN, F., DE LA LUNA, E., CAPPA, A., LIKIN, K., FERNÁNDEZ, A., TJ-II TEAM, Plasma Phys. Control. Fusion **45** (2003) 105.
- [17] DNESTROVSKIY, Y.N., MELNIKOV, A.V., LOPEZ-BRUNA, D., DNESTROVSKIY, A.Y., CHERKASOV, S.V., DANILOV, A.V., ELISEEV, L.G., KHABANOV, F.O., LYSENKO, S.E., SYCHUGOV, D.Y., Plasma Phys. Control. Fusion **65** (2023) 015011.
- [18] POPOV, A.Y., GUSAKOV, E.Z., Phys. Plasmas **31** (2024) 072104.